

PAPER • OPEN ACCESS

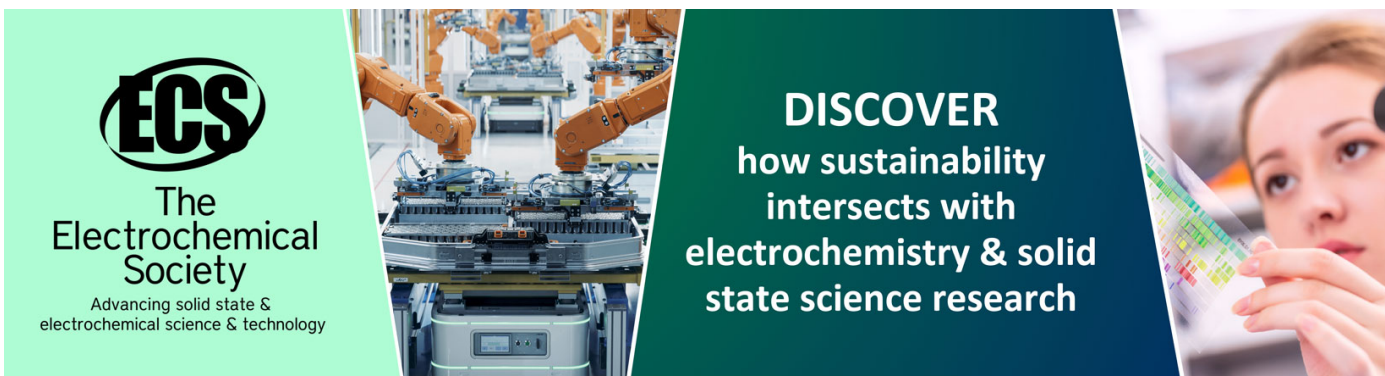
## Improvement Parameters for Design Brushless DC Motor by Moth Flame Optimization

To cite this article: Hanan A R Akkar and Sameem Abbas Salman 2020 *IOP Conf. Ser.: Mater. Sci. Eng.* **745** 012019

View the [article online](#) for updates and enhancements.

You may also like

- [Design and Realization of Control System of Brushless DC Motor Based on ARM](#)  
Jinjin Ye and Zhigong Huang
- [Application of Particle Swarm Optimization \(PSO\) Algorithm for PID Parameter Tuning in Speed Control of Brushless DC \(BLDC\) Motor](#)  
Pratap Bhandari, Basanta Pancha, Yam Krishna Poudel et al.
- [Hybridized GWO-RUN optimized fractional order control for permanent magnet brushless dc motor](#)  
Sweety Kumari and Ramesh Kumar



**ECS**  
The  
Electrochemical  
Society  
Advancing solid state &  
electrochemical science & technology

**DISCOVER**  
how sustainability  
intersects with  
electrochemistry & solid  
state science research

# Improvement Parameters for Design Brushless DC Motor by Moth Flame Optimization

Hanan A R Akkar<sup>1</sup> and Sameem Abbas Salman<sup>2</sup>

<sup>1,2</sup>Electrical Engineering Department, University of Technology, Baghdad, Iraq.

E-mail: 30080@uotechnology.edu.iq, bsceng2006@yahoo.com

**Abstract:** This contribution deals with an improved design of a brushless DC motor, using optimization algorithms, based on collective intelligence. For this purpose, the case study motor is perfectly explained and its significant specifications are obtained as functions of the motor geometric parameters. In fact, the geometric parameters of the motor are considered as optimization variables. Then, the objective function has been defined. This function consists of three terms; losses, construction cost and the volume of the motor which should be minimized simultaneously. The three algorithms are Moth Flame, Genetic and Particle Swarm have been studied in this paper. It is noteworthy that Moth flame optimization (MFO) algorithm has been used for the first time for brushless DC motor design optimization. A comparative study between the mentioned optimization approaches shows that moth flame optimization algorithm has been converged to optimal response in less than 250 iterations and its standard deviation is  $\pm 0.03$ , while the convergence rate of the genetic and particle swarm algorithms are about 400 and 450 iterations with standard deviations of  $\pm 0.07$  and  $\pm 0.06$ , respectively for the case study motor. The obtained results show the best performance for the Moth Flame Optimization algorithm among all mentioned algorithms in brushless DC motor design optimization.

## 1. Introduction

The use of DC motors has become common in the industry due to highlighted specifications such as vast speed control and high efficiency [1-3]. However, the presence of commutator and brushes can be considered as a major disadvantage of such motors due to constant erosion of the mentioned components which can finally lead to an increase in a safety hazard and the maintenance cost. But this problem has been solved by the use of brushless DC (BLDC) motors. In these motors, electric circuits have been applied instead of commutator and brushes [2, 4]. So far, several investigations have been conducted on the optimization of BLDC motor design. As stated in literature [5], a BLDC motor has been optimized by orthogonal multi-objective chemical reaction optimization algorithm (OMOCRO), to achieve maximum efficiency with the minimal material cost. Consequently, a comparative experiment among non-dominated sorting genetic algorithm, multi-objective particle swarm and OMOCRO shows the best performance of OMOCRO for BLDC motor design optimization.

A novel optimization method has been proposed in [6] with search region management (SRM) to improve the efficiency of the local search algorithms. The mentioned method has been tested for optimal design of a BLDC motor with the help of FEA to minimize the torque ripple. In [7], a Multi-objective Krill Herd algorithm (MOKH) using the beta distribution in the inertia weight tuning has been proposed for electromagnetic optimization of a BLDC Motor with a promising performance. The researchers in [8] has proposed the genetic algorithm for topology optimization of the stator teeth in a BLDC motor to reduce the torque ripple without decreasing the average torque. In [9], an optimized



BLDC motor through a population-based algorithm called interstellar search method (ISM) with mesh adaptive direct search has been proposed. The reduction of the torque ripple has been considered as the main objective of this paper. In [10], deals with the optimal design of an interior permanent magnet BLDC motor using cost-effective ferrite magnets to maximize the flux density and minimize the torque ripple. The genetic algorithm has been applied for flared shape rotor structure optimization. In [11], the researchers have optimized the anisotropic ferrite magnet shape and the magnetization direction of an interior permanent magnet BLDC motor to maximize back-EMF of the mentioned motor with the help of FEM. In [12], a 2-D analytical solution to predict the distribution of magnetic field and comparing the results with 2-D FEM in ironless BLDC motor, used in a flywheel. In [13], an outer rotor type motor design has been discussed that used in the blower system of a vehicle by a BLDC and also BLAC motor with the help of finite element analysis. In most of the literature mentioned that the influence of the required velocity has been ignored in optimization and as a result, the motor potential has not been nicely described [5-10]. On the other hand, the applied optimization approaches are based on simple analysis with sensitivity to initial conditions that have been widely used in recent years. Therefore, employing a more up to date optimization algorithm seems to be vital. This investigation gives an in-depth examination to represent the fundamental equations for BLDC motor design, considering both speed and torque as mechanical required parameters and using Moth flame optimization (MFO) as a suitable approach for motor optimal design. To this end, the geometric parameters of the motor are considered as the optimization variables. Then the objective function is defined, based on minimizing the losses, construction cost and the volume of the motor. Finally, the obtained results of the three optimization approaches have been compared and the MFO has been extracted as the best method.

## 2. Materials of a BLDC Motor and the Applied Methods

2.1. *BLDC Motor Structure:* Figure 1 depicts the structure of the studied motor in addition to its geometrical parameters [14]. Furthermore, the shown parameters in Figure 1 have been introduced in Table 1.

### 2.2. Design Features

2.2.1. *Electromagnetic Torque:* For obtaining the total torque, the specifications which depend on the body material of the BLDC motor such as filling factor of the coil ( $k_f$ ), permanent magnet and the stator and rotor core flux density ( $B_r$ ), should be given in the knee point of the B-H curve.

**Table 1.** Parameters of BLDC Motor

number of pole pairs = $P$	thickness winding = $l_w(m)$
cross sectional area of the winding = $A_c(mm^2)$	mechanical air gap = $l_g(m)$
poarc per p-lep-oleitch ratio = $\beta$	rotor radius = $r_r(m)$
magnet thickness = $l_m(m)$	current density = $J_{cu}(Am^{-2})$
thickness stator/rotor core = $l_y(m)$	wire gauge and stato/rotor axial length = $l_s(m)$

Assuming the conductor and the magnetic field are orthogonal to each other, the total torque can be obtained as follows [14, 15]:

$$T = A_w J_{cu} k_f k_c l B_r \quad (1)$$

$$A_w = \pi l_w (2r_r + 2l_g + l_w) \quad (2)$$

Where,  $l$  and  $k_c$  represent the length of the conductor and the correction factor, respectively and  $A_w$  is the cross section of the coil. no matter the armature response and additionally the reluctance of the stator and rotor core, the magnetic flux density might be as follows [14, 15]:

$$B_g = \frac{F_m}{A_g \mathcal{R}} = \frac{B_r l_m}{(r_r + l_g) \ln\left(\frac{r_r + l_g + l_w}{r_r - l_m}\right)} \quad (3)$$

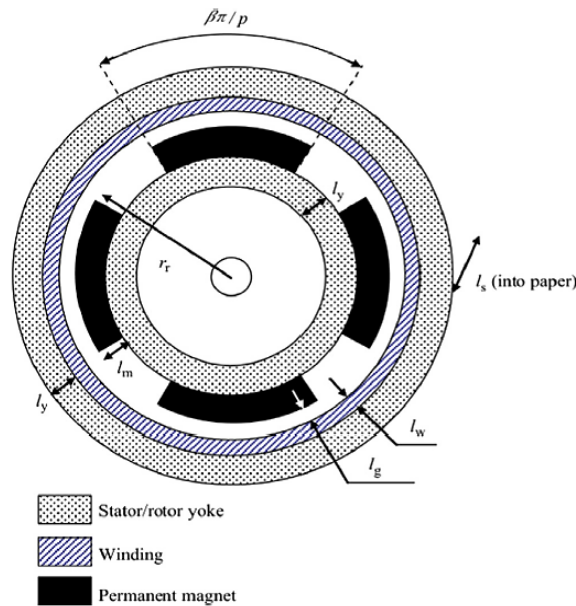


**Figure 1.** The Structure of the Studied BLDC Motor.

Where,  $F_m$  is the magneto-motive force and  $\mathcal{R}$  is the total reluctance of each winding.  $A_g$  Can be obtained as:

$$A_g = l_s \frac{\beta\pi}{p} (r_r + l_g) \quad (4)$$

The electromagnetic torque of the BLDC motor based on its geometric parameters can be expressed in accordance to Equation (5).

$$T_{em} = \frac{\pi k_f k_c k_l k_\beta B_r l_m l_s l_w (2r_r + 2l_g + l_w) J_{cu}}{\ln\left(\frac{r_r + l_g + l_w}{r_r - l_m}\right)} \quad (5)$$

The leakage component of the magnetic field ( $k_l$ ) and also the active area of the auxiliary coil and magnet ( $k_\beta$ ) are expressed with the help of Equation (6) and (7), respectively.

$$k_l = 1 - \frac{1}{0.9[r_r/(\beta p(l_g + l_w))]^2 + 1} \quad (6)$$

$$k_\beta = \frac{\alpha(\beta, k_c)}{k_c} \quad (7)$$

$\alpha$ , indicates extend of the active coils, locating in the PM magnetic field, as shown in Figure 2. This parameter can be approximated by the following equation.

$$\alpha = \min(\beta, k_c) [k_s + (1 - k_s)\tanh(\delta|\beta - k_c|)] \quad (8)$$

It is noteworthy that,  $k_s < 1$  and  $\delta$  is obtained by experience and testing.

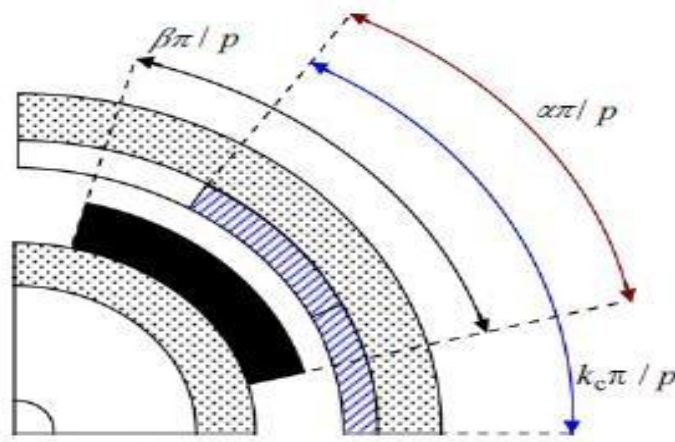


**Figure 2.** Concept of  $\alpha$

### 2. 2. 2. The Mechanical and Electrical Criteria

For making a relation between the motor geometry and the desired velocity, the electrical and also mechanical criteria should be defined in order to restrict the rotational velocity. From the mechanical aspect, the bearings are able to withstand high rotational speeds. Therefore, they hardly impose any limitation on rotational velocity. On the other hand, other rotating parts, especially permanent magnet can impose limitations on the maximum rotational velocity. As a result, a non-magnetic rotating sleeve is applied in order to enhance the mechanical robustness of the rotor.

From electrical point of view, the electrical time constant ( $\tau = L/R$ ), can limit the maximum rotational velocity.  $R$  and  $L$  represent the resistance and the inductance of each winding, respectively.

### 2. 2. 3. Cost of Materials

The volume of the applied materials, which depend on the motor geometry, have significant impacts on the motor cost as expressed in equation (9).

$$C = C_m + C_w + C_y \quad (9)$$

Where,  $C_m$ ,  $C_w$  and  $C_y$  represent the costs of permanent magnet, winding and stator/rotor core, respectively. Each term of equation (9), can be written in detail as follows.

$$C_m = c_{m1}\rho_m V_m + c_{m2}P \quad (10)$$

$$C_w = c_w A_g k_f \rho_w V_w \quad (11)$$

$$C_y = c_y \rho_y V_t \quad (12)$$

Where,  $c_{m1}$ ,  $c_w$  and  $c_y$  are the cost per unit mass of permanent magnet, winding and core materials, respectively.  $\rho_m$ ,  $\rho_w$  and  $\rho_y$  represent the mass densities of permanent magnet, winding and rotor/stator core, respectively. Finally,  $V_m$ ,  $V_w$  and  $V_t$  are the volumes of the permanent magnet, winding and rotor/stator core, respectively.

### 2. 2. 4. Losses in BLDC motors

Losses in BLDC motors are divided into three groups; electrical, magnetic and mechanical losses. The power loss due to resistance of windings can be obtained as follows.

$$P_{cu} = \rho k_f k_c k_{et} A_w l_s J_{cu}^2 \quad (13)$$

On the other hand, the eddy current and hysteresis losses are considered as two major magnetic losses of a BLDC motor.

Assuming equal magnetic flux of the air-gap and the core, the maximum magnetic density of the stator is expressed as [14].

$$B_{sy} = \frac{\pi k_1 \beta B_r l_m}{2pl_y \ln \left[ \frac{r_r + l_g + l_w}{r_r - l_m} \right]} \quad (14)$$

Thus, the following equations are obtained for eddy current and hysteresis losses, respectively.

$$P_e = k'_e \rho_y V_{sy} B_{sy}^2 f^2 \quad (15)$$

$$P_h = k'_h \rho_y V_{sy} B_{sy}^n f \quad (16)$$

Where,  $\rho_y$  is the density of the motor material and  $V_{sy}$  represents the stator volume. It should be noted that, the frequency in equations (15) and (16) is calculated in accordance to equation (17).

$$f = \pi w_r / 2\pi \quad (17)$$

On the other side, the mechanical losses in a BLDC motor can be divided into two categories including; friction and wind age. The friction losses can be written as follows [14].

$$P_b = \frac{N_b}{2} \mu_f F_b d_i \omega_r \quad (18)$$

Where,  $F_b$  and  $d_i$  are the load and the internal radius of the bearing. On the other hand,  $\mu_f$  and  $N_b$  represent the bearing friction factor and the number of bearings respectively. The wind age losses can be obtained as follows.

$$P_w = \pi k_r C_f \rho_{air} \omega_r^3 r_r^4 l_s \quad (19)$$

Where,  $k_r$  and  $\rho_{air}$  represent the roughness factor of the rotor and the air density respectively and  $C_f$  is the friction factor which is obtained by Equation (20) in which  $Re$  is the Couette-Reynolds number.

$$C_f = \begin{cases} 0.5150 \frac{(l_g/r_r)^{0.3}}{Re^{0.5}} & \text{for } 500 < Re < 10^4 \\ 0.0325 \frac{(l_g/r_r)^{0.3}}{Re^{0.2}} & \text{for } 10^4 < Re \end{cases} \quad (20)$$

$$Re = \rho_{air} w_r r_r l_g / \mu_{air}$$

$$T_{em} = \frac{\pi k_f k_c k_1 k_\beta B_r l_m l_s l_w (2r_r + 2l_g + l_w) J_{cu}}{\ln \left[ \frac{r_r + l_g + l_w}{r_r - l_m} \right]} - \frac{P_e + P_h}{w_r} \quad (21)$$

$$T_{out} = T_{em} - (P_w + P_b) / \omega_r \quad (22)$$

In accordance to the obtained magnetic and mechanical losses, the modified formula of the electromagnetic and also the output torque can be modified as equations (21) and (22). Also, the total losses of a BLDC motor can be expressed as:

$$P_{total} = P_{cu} + P_e + P_h + P_b + P_w \quad (23)$$

### 3. Optimization Methods

This paper applies three different evolutionary algorithms, MFO [16], Genetic Algorithm (GA) [17, 18] and Particle Swarm Optimization (PSO) [19-21], for optimal design of the BLDC motor. GA is a popular applied algorithm because of several reasons such as, its high intuitiveness, ease of implementation, its high capability to solve highly nonlinear mixed integer optimization problems, large number of parameters and obtaining multiple local optima. On the other hand, PSO, has the same advantages as GA, but with better computational efficiency by applying statistical analysis and formal hypothesis testing. But this study has applied the MOF for optimal design of BLDC motor for the first

time. The MFO algorithm has superiority to many other optimization algorithms such as GA and PSO, typically for multi-objective functions. In MFO, the local search is performed with higher efficiency because there is only a single parameter apart from the population. In fact the only parameter which should be adjusted is the fraction of the nests needed to be abandoned (Pa). This issue improves the computing power and speed. GA and PSO are common algorithms and have been completely described in references [17- 21]. But since, MFO, has been used as the main algorithm for motor optimal design in this study, an initial understanding from the concept of these algorithms is presented as follows.

### 3.1. Moth Flame Optimization Algorithm

MFO is an optimization algorithm inspired from the navigation method of Moths. Moths using transverse orientation techniques for navigation at night by keeping a fixed angle with the moonlight direction, so that Moths can move for long distances in a straight path. For modeling, the Moth transverse orientation, suppose that the Moths represent the problem candidate solutions and the position of Moths represent the variables of the problem, while the flame indicates the best position of each Moth obtained by iteration. Like other population-based metaheuristic algorithms, MFO begins with a random population in the search space, evaluate the best initial solution according to fitness function then updating Moth's position according to spiral movement of the Moths as follows:

$$\mathbf{x}_i^{j+1} = \mathbf{AD}_i^j e^{(\epsilon c)(\alpha r)} \cos(2\pi(\alpha r)) + \mathbf{f}_k^j \quad (24)$$

$$\mathbf{AD}_i^j = |\mathbf{f}_k^j - \mathbf{x}_i^j| \quad (25)$$

Where  $\mathbf{x}_i^j$  indicates the  $i$ th moth at  $j$ th iteration,  $\mathbf{f}_k$  indicates the  $k$ th flame, both Moth and flames are candidate solution, but flames are the local best position of Moths,  $\mathbf{AD}_i$  indicates the distance between the  $i$ th Moth and the  $k$ th flame,  $\epsilon c$  is a constant used for the shape of the spiral movement, and  $\alpha r$  is a random number  $\in [Rc, 1]$  and represents how much moth close to a flame to ensure further moth exploitation,  $Rc$  represents convergence constant that linearly reduced from -1 to -2 over an epoch of iterations. Equation (24), describes how Moths modify their positions, but not essentially in space between flames [16].

To prevent MFO trapped into local minima position, each Moth is binding to modify its position according to only one of the sorted flames, where after each iteration flames are arranged according to their fitness. The number of flames is reduced over the epoch of iterations as shown in equation (26), due to the fact that the updating of Moths position according to different locations in the space may decrease the exploitation of the best solutions.

$$\mathit{nof} = \mathit{round}\left(\mathit{f}_{\max} - j \frac{(\mathit{fl}_{\max} - 1)}{\mathit{maxit}}\right) \quad (26)$$

Where  $\mathit{fl}_{\max}$  represents the maximum number of flames,  $j$  is the current iteration number,  $\mathit{maxit}$  is the maximum iteration number [16]. Table 2 illustrates the MFO algorithm pseudo code.

**Table 2** General MFO Pseudo Code.

- 
- 1: Generate initial random population (initialization of individuals), and initial parameters.
  - 2: Evaluate the fitness of the moths.
  - 3: While not (population converge to optimum solution or maximum iteration reached)
  - 4: Use Equation (26) to evaluate the flames number.
  - 5: According to iteration number sort flames and flame fitness.
  - 6: For  $i=1: M$
-

- 
- 7: For  $k=1: N$
- 8: Update  $Rc$  and  $\alpha r$
- 9: Use Equation (25) to evaluate  $AD$  according to the corresponding moth and flame.
- 10: Modify moths using Equation (24)
- 11: End
- 12: End
- 13: Loop (next generation).
- 

### 3.2. Determination of the effective parameter for the optimization methods.

Accordance to literatures [16-21], the determinate parameters of the optimization algorithms are introduced. This parameters are  $f_k$  and  $\alpha r$  for MFO; the cross over rate and also the percentage of mutation for GA and ( $C_1$ & $C_2$ ) for PSO. ( $C_1$ & $C_2$ ) determine the travelled distance of a particle in each iteration [19-21]. The amount of the aforementioned parameters of the optimization algorithms, are measured in 20 different conditions. Each measurement is implemented individually for about 50 times and finally, the effective parameters, mentioned in Table 3, are obtained from the eights, twentieth and fourth implementation of MFO, GA and PSO, respectively.

**TABLE 3.** The value of effective optimization parameters

MFO		GA		PSO	
$f_k$	$\alpha r$	Cross over rate	Mutation (%)	$C_1$	$C_2$
30	[-1,1]	0.8	0.1	1.6	2

## 4. Optimization Problem Data

### 4.1. Design Variables and Constant Values

The optimization variables are those parameters of the case study motor that should be optimized. These parameters are presented in the following vector.

$$\mathbf{x} = [\mathbf{p} \ \boldsymbol{\beta} \ l_m \ l_y \ l_w \ l_g \ l_s \ r_r \ J_{cu} \ A_c]^T \quad (27)$$

Generally, there are 10 different design variables that should be optimized. Other quantities such as power losses, output torque, costs and volume of the motor can be calculated through them. The aforementioned design variables were defined in Table 1. while, the constant parameters of this motor are presented in Table 4.

### 4.2. Objective Function, with Considering the Constraints.

An appropriate definition of the objective function with consideration to the constraints is always known as the most significant issue in solving any optimization problem. The main concern in this investigation includes reduction of the cost, volume and power loss of a BLDC motor. For this reason, the objective function will be as follows:

$$f_o(\mathbf{x}) = w_v V_t(\mathbf{x}) + w_p P_{total}(\mathbf{x}) + w_c C(\mathbf{x}) \quad (28)$$

Where,  $C(\mathbf{x})$ ,  $P_{total}$  and  $V_t(\mathbf{x})$  represent, cost function, power loss function and volume function of the motor, respectively. On the other hand,  $w_c$ ,  $w_p$  and  $w_v$  are the related weight of cost function, power loss function and volume function of the motor. In fact, these coefficients clarify the impact of each function. In addition to electrical and mechanical constraints, some other limitations such as thermal, cost and manufacturing constraints are of great importance. The only electrical constraint is the

voltage which can be obtained with appropriate selection of the winding diameter. Similarly, the mechanical constraints can be expressed as follows.

$$\begin{cases} T_{em} \geq T_{em}^* \\ \omega_r^{max} \geq \omega_r^* \end{cases} \quad (29)$$

Where,  $T_{em}^*$  and  $\omega_r^*$  are arbitrary torque and speed respectively.  $\omega_r^{max}$  is considered as the maximum speed in the arbitrary torque. It should be noticed that, the manufacturing constraints contain some parameters such as minimum air-gap ( $l_g^{min}$ ) and the minimum area of the section ( $A_c^{min}$ ). Other constraints, caused by thermal limitations and saturation effect, are expressed as follows.

$$\begin{cases} B_{sy} \leq B_{sy}^{knee} \\ k_f I_w J_{cu}^2 \leq k \end{cases} \quad (30)$$

Where,  $B_{sy}^{knee}$  represents the magnetic flux density at the knee point of the B-H curve and k is the maximum permissible temperature of the windings. After considering the impact of the electromagnetic torque, speed and magnetic flux density constraints, the objective function has been modified as follows.

$$\begin{aligned} f_o(x) = & w_v V_t(x) + w_p P_{total}(x) + w_c C(x) \\ & + \frac{1}{\varepsilon} \left[ f_u \left( 1 - T_{em} / T_{em}^* \right) + f_u \left( 1 - \omega_r^{max} / \omega_r^* \right) \right. \\ & \left. + f_u \left( B_{sy} / B_{sy}^{knee} - 1 \right) \right] \end{aligned} \quad (31)$$

$$f_u(x) = \frac{1}{1 + e^{-\sigma x}}$$

Where,  $\varepsilon$  is a tiny amount and  $\sigma$  is considered as a constant large number.

**Table 4.** Constant parameters of the BLDC motor

Quantity	Amount	Quantity	Amount
$k_f$	0.7	$w_p$	0.02
$k_c$	0.666	$w_v$	2000/3
$k_s$	0.95	$w_c$	0.0125
$k_r$	1	$\rho_m (kg m^{-3})$	7400
$\delta$	5	$\rho_w (kg m^{-3})$	8900
$B_r (T)$	1	$\rho_y (kg m^{-3})$	7700
$B_{sy}^{knee} (T)$	1.5	$c_{m1} (\text{£ } kg^{-1})$	20
$K (A^2 m^{-3})$	$10^{11}$	$c_{m2} (\text{£ } kg^{-1})$	1
$\rho (\Omega m)$	$1.8 \times 10^{-8}$	$c_y (\text{£ } kg^{-1})$	3
$k'_h (W s kg^{-1} T^{-n})$	$0.018^a$	$c_1 (\text{£ } m^2 kg^{-1})$	0.045
$k'_e (W s^2 kg^{-1} T^{-2})$	$0.00008^a$	$c_2 (\text{£ } m^2 kg^{-1})$	5.42
$n$	$1.92^a$	$T_{em}^* (Nm)$	10

$\gamma$	1	$w_r^*(rad\ s^{-1})$	157
$V^*(v)$	140		

#### 4. 3. Summary and Discussion

For implementation of the BLDC motor optimization problem, the significant specifications of the motor are obtained as functions of the motor geometric parameters. The geometric parameters are mentioned in Table.1. In fact the mentioned parameters of the motor are considered as optimization variables and other quantities i.e. power losses, output torque, costs and volume of the motor can be calculated and optimized through them. The objective function consists of three terms including, losses, motor volume and manufacturing cost. The cost term is calculated by Equation (9), this Equation can be written in detail in accordance to Equations (10)-(12). Equations (3) and (4) are needed to define Equation (11). The total losses of a BLDC motor can be expressed as Equation (23). This equation has 5 terms including, Equations (13), (15), (16), (18) and (19). Equation (14) is essential for defining Equations (15) and (16) and also Equation (20) is necessary for defining Equation (19). For clarifying the impact of each function the related weight of cost function, power loss function and volume function of the motor is considered as in Equations (28). Equations (29) and (30) express the constraints of the objective function. By considering the constraints in Equation (28), the final objective function is shown as Equation (31). By means of optimization algorithms which are implemented on Equation (31), the geometric parameters and also the volume of the motor will be optimal in addition to losses and manufacturing cost simultaneously.

### 5. Simulation Results and Discussion

#### 5.1. Technical Analysis of the Optimized Parameters

After implementation of the algorithms according to the effective parameters, mentioned in subsection 3.2; design variables and constant values, mentioned in subsection 4.1 and also the modified objective Function, presented in subsection 4.2, the optimal parameters of the case study motor are obtained. These values along with the minimum and maximum values of the parameters are given in Table 5. It should be noted that, GA and PSO results are validated with reference [14]. According to Table 5, when MFO is applied, most of the geometrical optimized parameters i.e.  $\beta$ ,  $l_m$ ,  $l_w$ ,  $l_g$  and  $l_s$  have the lowest values. Therefore, the motor has the lowest possible volume and lowest cost. On the other hand, the cross-sectional area of the winding and the current density ( $A_c$  and  $J_{cu}$ ) are also more applicable.

**Table 5.** Limitations and Optimal Value of Motor

No	Parameters	Min	Max	MFO	GA	PSO
1	$\beta$	0.5	1	0.5912	0.7	0.6950
2	$l_m(m)$	0.001	0.015	0.0090	0.0130	0.0124
3	$l_y(m)$	0.002	0.01	0.0031	0.0060	0.0058
4	$l_w(m)$	0.001	0.0055	0.0013	0.0035	0.0034
5	$l_g(m)$	0.001	0.004	0.001	0.001	0.001
6	$r_r(m)$	0.005	0.1	0.0492	0.0595	0.059
7	$l_s(m)$	0.006	0.6933	0.0630	0.0756	0.0732
8	$A_c(mm^2)$	0.1	2	1.7551	2	1.9982
9	$J_{cu}(Am^{-2})$	$3 \times 10^6$	$6 \times 10^6$	5924600	5800000	5784573

As a result, the objective function has the best value, using MFO, as presented in Table 6. Another significant issue in any optimization approach is the convergence rate of the algorithm. The MFO, converged after 250 iteration while the GA and PSO converge after 400 and 450 iterations, respectively. This issue indicates the suitable convergence rate of MFO.

**TABLE 6.** Specifications of the optimized BLDC motor

NO	Parameters	MFO-Value	GA-Value	PSO-Value
1	$V_t(m^3)$	0.0011	0.00536	0.0042
2	C (£)	63.6417	68.86	66.51
3	$P_{total} (W)$	51.2446	56.71	54.3
4	$P_{cu} (W)$	41.1851	44.81	42.69
5	$P_h (W)$	4.4115	6.18	6.04
6	$P_e (W)$	2.4500	3.52	3.76
7	$P_b (W)$	1.1195	2.12	2.53
8	$P_w (W)$	0.0683	0.09	0.0797
9	$W_p V_t$	0.5891	0.836	0.75
10	$W_c C$	0.6205	0.861	0.704
11	$W_p P_t$	1.0248	1.536	1.843
12	$f_o$	2.39	3.78	2.61
13	Efficiency	97.61%	94.26%	95.38%

14	Standard	$\pm 0.03$	$\pm 0.07$	$\pm 0.06$
15	V (Volt)	150.36	141.1	136
16	I (Ampere)	11.6115	11.6	11
17	$P_{out}$ (W)	1642	1450	1521.31

### 5. 2. The Impact of Motor Geometrical Parameters on the Objective Function

Figure 3 shows the variation of the objective function, due to changing each geometrical parameter of the motor, while the rest of parameters remain constant. This figure is divided into 9 subfigures and is labeled from (a) to (i). Each subfigure depicts the impact of changing each geometrical parameter of the motor i.e.  $P$ ,  $\beta$ ,  $l_m$ ,  $l_w$ ,  $l_g$ ,  $l_s$ ,  $l_y$ ,  $r_r$  and  $J_{cu}$  on the objective function, respectively. In all the subfigures, the red line, blue line and green point represent the proposed objective function variation, unconstrained objective function and the optimal point, respectively.

In accordance to Figure 3a, the large number of poles causes an increment in the motor manufacturing cost and also a decrement in the magnetic losses due to low density of magnetic flux in stator and rotor core. It should be noted that, this issue has no impact on the volume of the motor. By considering the proposed objective function and Figure 3a, it is concluded that, applying higher number of poles can lead to a better design of the motor. However, this issue causes an increment in the leakage magnetic flux and a decrement in the output torque. According to Figure 3b, the value of  $\beta$  has no effect on the volume of the motor. But it is noteworthy that, a lower value of  $\beta$  can lead to a reduction in the cost, magnetic leakage flux, magnetic losses and also the output torque. On the other hand, a large value of  $\beta$  can lead to a decrement in the output torque due to its effect on increasing the magnetic leakage flux. Figure 3c shows that, reduction of  $l_m$  leads to improvement of manufacturing cost, volume and losses of the BLDC motor. But on the other hand, the output torque and the maximum speed of the motor still keep decreasing as before. As shown in Figure 3d, an increment in  $l_y$  will lead to a reduction in

the magnetic losses and causes an increment in the cost and volume of the motor. It should be noted that, considering a very small value for  $l_y$ , may lead to saturation. Figure 3e, shows that, the existence of high space for winding has different impacts on the cost and volume of the motor. But in general, it can lead to improvement of the efficiency. It is noteworthy that,  $l_w$  should not be lower than a permissible amount. Otherwise, the motor will not be able to produce a suitable torque. The radius of the rotor  $r_r$  is considered as one of the most significant parameters in a BLDC motor design. As shown in Figure 3f, by reducing the  $r_r$  value, all the three items in the objective function will be reduced simultaneously. But it should be noted that, a very small  $r_r$  value has negative effect on producing the necessary output torque and on the other hand, a very larger  $r_r$  value has inverse effect on the maximum speed of the motor. Figure 3g depicts that, a small value of  $l_g$  is favorable, but unfortunately, this small amount can lead to an adverse impact on the output torque of the motor. This issue is not desirable. As shown in Figure 3h,  $l_g$  which shows the air-gap amount, is considered to have its minimum value. Figure 3i indicates that, the output torque and the copper losses are proportional to the current density and the square of current respectively. Although, increasing the current density can lead to an improvement in the cost and volume of the motor, but it is noteworthy that, the impact of an increment in the copper losses is able to overcome the two aforementioned advantages.

### 5. 3. The Comparison of MFO Performance with GA and PSO

Figures 3, 4, 5 and Table 7 shows the convergence rate, fitness, the standard deviation of MFO, GA and PSO algorithms and also MFO, GA and PSO training flowchart.

**Table 7.** The comparison of applied methods

Algorithm	Fitness	Standard deviation	Convergence rate
MFO	1.59	$\pm 0.03$	250
GA	2.78	$\pm 0.07$	400
PSO	2.71	$\pm 0.06$	450

By considering, Table 7 and Figure 4, it is concluded that, MFO algorithm has the best performance among all the described algorithms for improvement parameters for design of a BLDC motor.

## 6. Conclusion

In this paper, an optimal design of a BLDC motor, using three optimization approaches i.e. MFO, GA and PSO has been studied. The priorities of parameters optimization in design of a motor are different in various applications. Therefore, the importance of this problem has become more obvious due to simultaneous parameter optimization. This investigation firstly clarifies significant specifications of the motor as functions of the motor geometric parameters. Then, the objective function has been defined in order to minimize the losses, construction cost and the volume of the motor simultaneously. Three different optimization approaches i.e. MFO, GA and PSO have been applied for the case study motor optimal design. It is noteworthy that, MFO has been used for the first time for this purpose. The obtained results of three optimization methods have been compared together and finally it is concluded that, MFO can converge to an optimal response in less than 250 iterations, while this value is 400 and 450 iterations for GA and PSO, respectively. As a result, the proposed method has an acceptable convergence rate. On the other hand, the obtained fitness value and the standard deviation of MFO is more applicable, compared with GA and PSO.

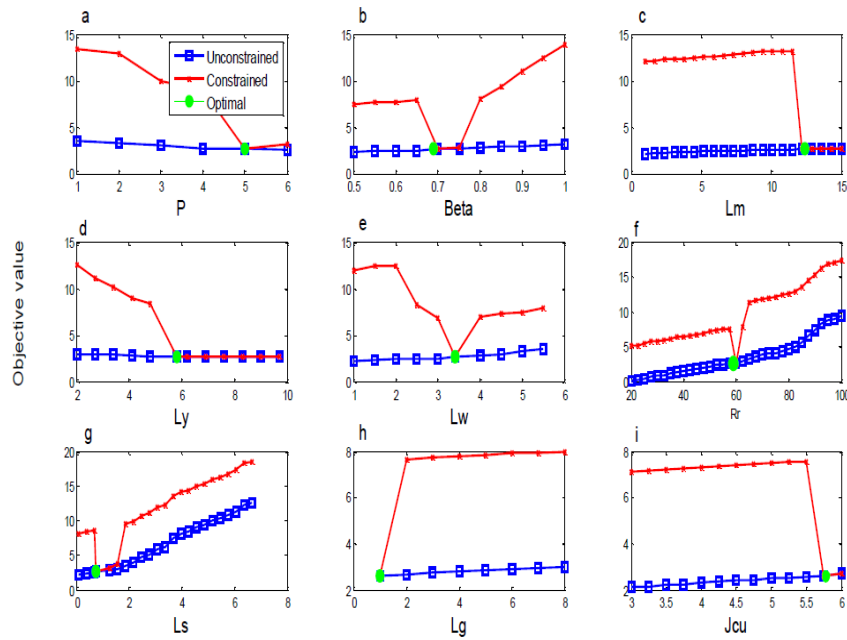


**Figure 3.** Objective function variation, due to changing each geometrical parameter of the BLDC motor.

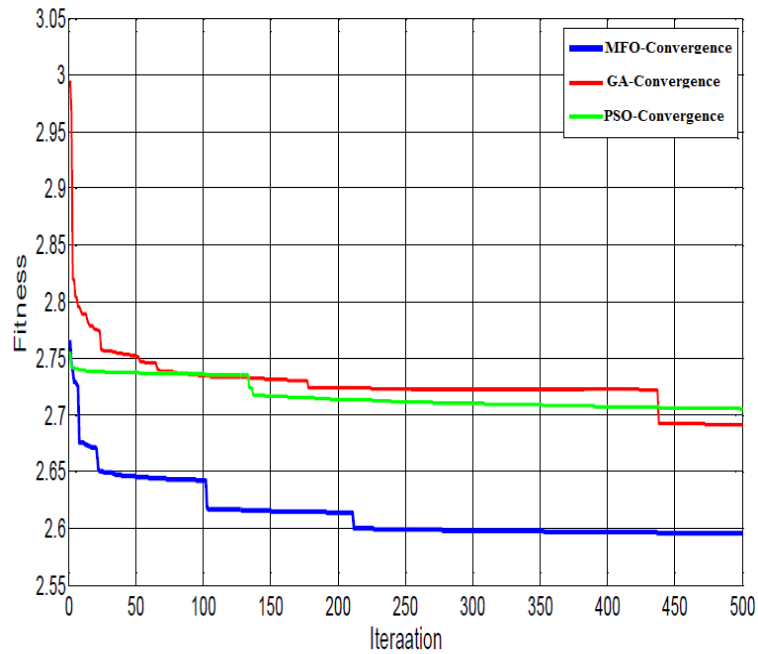


**Figure 4.** The convergence waveform comparison of MFO, GA and PSO.

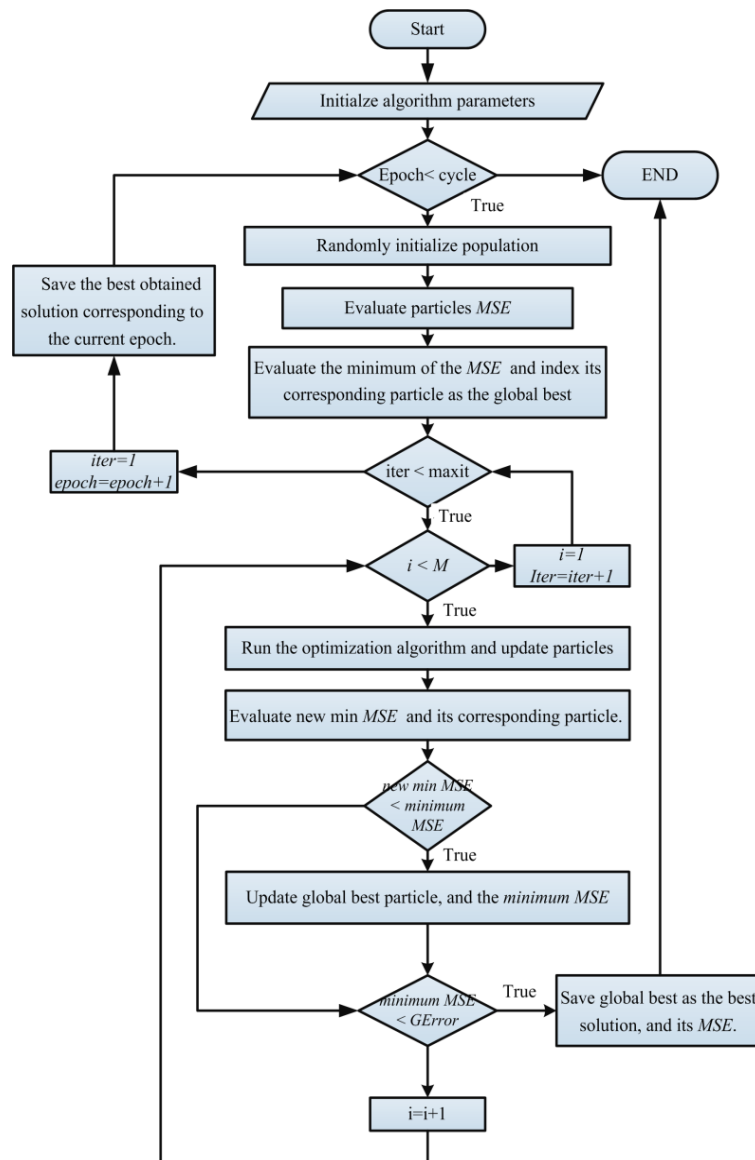


**Figure 5.** MFO, GA and PSO training flowchart.

## 7. References

- [1]. Juha Pyrhonen ,Tapani Jokinen ,Valeria Hrabovcova,. 2009 "*Design of rotating electrical machines*", *John Wiley & Sons, E-Book*.
- [2]. Qingping Wu ,Wenchao Tian., 2012 "Design of Permanent Magnet Brushless DC Motor Control System Based on DSPIC30F4012 ", *Procedia Engineering*, vol. 29, pp. 4223-4227.
- [3]. Neeraj Priyadarshi ,Sanjeevikumar Padmanaban , et al .2018 "Maximum Power Point Tracking for Brushless DC Motor-Driven Photovoltaic Pumping Systems Using a Hybrid ANFIS-FLOWER Pollination Optimization Algorithm". *Energies*, vol. 11, no. 5, pp. 1067.
- [4]. Ahmed Rubaai , Paul Young, 2016 "Hardware/software implementation of fuzzy-neural-network self-learning control methods for brushless DC motor drives", *IEEE Transactions on Industry Applications*, vol. 52, no. 1, pp. 414-424.
- [5]. Haibin Duan, Lu Gan. 2015 "Orthogonal multiobjective chemical reaction optimization approach for the brushless DC motor design", *IEEE Trans. on Magnetics*, vol. 51, no. 1, pp. 1-7.

- [6]. Tae-Yong Lee, Pham Xuan Trung, Jong-Wook Kim, Yong-Jae Kim, Sang-Yong Jung. 2016 "Search region management method for local search algorithm employing design optimization of brushless dc motor", *IEEE Trans. on Magnetics*, vol. 52, no. 3, pp. 1-6.
- [7]. Helon V. H. Ayala , Emerson H. V. Segundo , et al., 2016 "Multiobjective krill herd algorithm for electromagnetic optimization", *IEEE Trans. on Magnetics*, vol. 52, no. 3, pp. 1-4.
- [8]. Takeo Ishikawa , Kouki Yonetake , Nobuyuki Kurita., 2011 "An optimal material distribution design of brushless DC motor by genetic algorithm considering a cluster of material", *IEEE Trans. on Magnetics*, vol. 47, no. 5, pp. 1310-1313.
- [9]. ByungKwan Son , Gyeong-Jae Park , et al., 2016 "Interstellar search method with mesh adaptive direct search for optimal design of brushless DC motor", *IEEE Trans. on Magnetics*, vol. 52, no. 3, pp. 1-4.
- [10]. Keun-Young Yoon , Byung-II Kwon., 2016 "Optimal design of a new interior permanent magnet motor using a flared-shape arrangement of ferrite magnets", *IEEE Trans. on Magnetics*, vol. 52, no. 7, pp. 14.
- [11]. Hong-seok Kim , Yong-Min You , Byung-il Kwon., 2013 "Rotor shape optimization of interior permanent magnet BLDC motor according to magnetization direction", *IEEE Transactions on Magnetics*, vol. 49, no. 5, pp. 2193-2196.
- [12]. Xiangdong Liu , Hengzai Hu , et al., 2016 "Analytical solution of the magnetic field and emf calculation in ironless BLDC motor", *IEEE Transactions on Magnetics*, vol. 52, no. 2, pp. 1-10.
- [13]. Tae-Yong Lee , Myung-Ki Seo , et al., 2016 "Motor design and characteristics comparison of outer-rotor-type BLDC motor and blac motor based on numerical analysis", *IEEE Transactions on Applied Superconductivity*, vol. 26, no. 4, pp. 16.
- [14]. A.Rahideh, T.Korakianitis, et al., 2010 "Optimal brushless DC motor design using genetic algorithms", *Journal of Magnetism and Magnetic Materials*, vol. 322, no. 22, pp. 3680-3687.
- [15] S. M. Sharkh, Lai., 2006 "Design optimisation of a slotless brushless permanent magnet DC motor with helically-wound laminations for underwater rim-driven thrusters", *University of Southampton*.
- [16]. Seyedali Mirjalili., 2015 " Moth-Flame Optimization Algorithm: A Novel Nature-inspired Heuristic Paradigm," *Elsevier Inc., Knowledge-Based Systems*, vol. 89, pp. 228–249.
- [17]. Ramin Salehi Arashloo, Jose Luis Romeral Martinez, et al., 2014 "Genetic algorithm-based output power optimisation of fault tolerant five-phase brushless direct current drives applicable for electrical and hybrid electrical vehicles", *IET Electric Power Applications*, vol. 8, no. 7, pp. 267-277.
- [18]. B.K.Sarkar,P.Mandal, et al., 2013 "GA-optimized feedforward-PID tracking control for a rugged electrohydraulic system design", *ISA Transactions*, vol. 52, no. 6, pp. 853–861.
- [19]. Chookiat Kiree,Danupon Kumpanya, et al., 2016 "PSO-based optimal PI(D) controller design for brushless DC motor speed control with back EMF detection", *Journal of Electrical Engineering & Technology*, Vol. **11**, No. 3, pp. 715–723.
- [20]. H.E.A.Ibrahim,F.N.Hassan, Anas O Shomer., 2014 "Optimal PID control of a brushless DC motor using PSO and BF techniques". *Ain Shams Eng. J.*, vol. 5, pp. 371–398.
- [21]. Neeraj Priyadarshi,P. Sanjeevikumar, et al., 2018 "A Fuzzy SVPWM Based Inverter Control Realization of Grid Integrated PV-Wind System with FPSO MPPT Algorithm for a Grid-Connected PV/Wind Power Generation System: Hardware Implementation". *IET Electr. Power Appl.*, vol. 12, pp. 962–971.